Hierarchical Self-Assembly of pH-Responsive Nanocomposites with Molecular-Scale and Mesoscale Periodicities

Le-Le Li,[†] Chen-Jie Fang,[‡] Hao Sun,[†] and Chun-Hua Yan*,[†]

Beijing National Laboratory for Molecular Sciences, State Key Laboratory of Rare Earth Materials Chemistry and Applications and PKU-HKU Joint Laboratory in Rare Earth Materials and Bioinorganic Chemistry, Peking University, Beijing 100871, and School of Pharmaceutical and Chemical Biology, Capital Medical University, Beijing 100069, China

Received January 28, 2008. Revised Manuscript Received June 3, 2008

We have demonstrated a novel synthesis of mesoscopically ordered stimulus-responsive silica-based hybrid materials through a hierarchical self-assembly process. Two cationic surfactants with a special functional chromophoric group at one end of a carbon chain and a trimethylammonium headgroup at the other end were synthesized and used as both structure-directing agents and functional nano building blocks. Using these two cationic ammonium surfactants with different chromophoric groups at their hydrophobic tails, the micrometer-sized particles with a two-dimensional hexagonal mesostructure and spherical particles with a wormlike mesostructure were produced, respectively. Both of the mesostructured composite particles exhibit strongly fluorescent and pH-responsive behaviors with a rapid and recyclable signal response. Significantly, the symmetry of the self-assembled architecture demonstrated here not only guarantees a high filling and total homogeneous distribution of organic functionalities but also affords precise molecular-scale control over the spatial distribution of the organic component in the mesoscopically ordered inorganic network, which endows the hierarchical materials with mechanical robustness, improved thermal stability, and faster responses to chemical stimuli.

Introduction

As we have learned from natural materials such as bone and seashells, hard (inorganic)/soft (organic) materials in periodic architectures can provide both useful functionality and mechanical integrity. For many applications, including catalysis, electronics, and their use as structural and biomedical materials, chemists in materials science seek to elaborate inorganic−organic composites and copy the properties of such natural materials. In particular, functional hybrid organic−inorganic nanocomposites, which offer a wide range of possibilities for preparing tailor-made materials in terms of chemical and physical properties, also present other advantages for designing materials for optical applications (versatile and facile chemistry, easy shaping and patterning, good mechanical integrity, and excellent optical quality).[1,2] However, it has proven difficult to organize and integrate inorganic and organic composites efficiently and controllably on the nanoscale.

In recent years, mesoporous silica materials[3,4] with a stable mesostructure, large surface areas, good biocompatibility, and a tailorable size of the mesopores on the nanometer scale have attracted considerable interest as hosts for development of organic−inorganic hybrid materials.[5] These host−guest materials combine the high stability of the inorganic host system and a new structure-forming mechanism due to the confinement of the guests in well-defined pore channels. Mesoporous silica used as a host can serve to protect, stabilize, and orient the organic moiety inside, meanwhile allowing its optical properties to be probed from outside because silica is chemically stable, inert, and optically transparent. Optically active dye incorporated silica-based hybrid materials have been suggested for fundamental studies such as the spectroscopy of isolated dye molecules in a mesostructure,[6] energy transfer in solids,[7] and the following

* To whom correspondence should be addressed. Fax: +86-10-6275-4179. E-mail: yan@pku.edu.cn.
[†] Peking University.
[‡] Capital Medical University.

(1) (a) Sanchez, C.; Lebeau, B.; Chaput, F.; Boilot, J. P. *Adv. Mater.* **2003**, *15*, 1969. (b) Katagiri, K.; Hamasaki, R.; Ariga, K.; Kikuchi, J. *J. Am. Chem. Soc.* **2002**, *124*, 7892. (c) Zhang, J.; Coombs, N.; Kumacheva, E. *J. Am. Chem. Soc.* **2002**, *124*, 14512. (d) Zhao, L.; Loy, D. A.; Shea, K. J. *J. Am. Chem. Soc.* **2006**, *128*, 14250. (e) Cho, B. K.; Jain, A.; Gruner, S. M.; Wiesner, U. *Chem. Mater.* **2007**, *19*, 3611. (f) Driesen, K.; Deun, R. V.; Görller-Walrand, C.; Binnemans, K. *Chem. Mater.* **2004**, *16*, 1531.
(2) (a) Carrington, N. A.; Xue, Z. L. *Acc. Chem. Res.* **2007**, *40*, 343. (b) Burns, A.; Owb, H.; Wiesner, U. *Chem. Soc. Rev.* **2006**, *35*, 1028.
(3) Kresge, C. T.; Leonowicz, M. E.; Roth, W. J.; Vartuli, J. C.; Beck, J. S. *Nature* **1992**, *359*, 710.
(4) Zhao, D.; Feng, J.; Huo, Q.; Melosh, N.; Fredrickson, G. H.; Chmelka, B. F.; Stucky, G. D. *Science* **1998**, *279*, 548.
(5) (a) Scott, B. J.; Wirnsberger, G.; Stucky, G. D. *Chem. Mater.* **2001**, *13*, 3140. (b) Moller, K.; Bein, T. *Chem. Mater.* **1998**, *10*, 2950. (c) Soler-Illia, G. J. d. A. A.; Sanchez, C.; Lebeau, B.; Patarin, J. *Chem. Rev.* **2002**, *102*, 4093. (d) Hoffmann, F.; Cornelius, M.; Morell, J.; Fröba, M. *Angew. Chem., Int. Ed.* **2006**, *45*, 3216. (e) Sanchez, C.; Boissière, C.; Grosso, D.; Laberty, C.; Nicole, L. *Chem. Mater.* **2008**, *20*, 682.
(6) (a) Gago, S.; Fernandes, J. A.; Rainho, J. P.; Ferreira, R. A. S.; Pillinger, M.; Valente, A. A.; Santos, T. M.; Carlos, L. D.; Ribeiro-Claro, P. J. A.; Gonçalves, I. S. *Chem. Mater.* **2005**, *17*, 5077. (b) Peng, C.; Zhang, H.; Yu, J.; Meng, Q.; Fu, L.; Li, H.; Sun, L.; Guo, X. *J. Phys. Chem. B* **2005**, *109*, 15278. (c) Thomas, A.; Polarz, S.; Antonietti, M. *J. Phys. Chem. B* **2003**, *107*, 5081. (d) Jung, C.; Hellriegel, C.; Platschek, B.; Wöhrle, D.; Bein, T.; Michaelis, J.; Bräuchle, C. *J. Am. Chem. Soc.* **2007**, *129*, 5570.

10.1021/cm800293y CCC: $40.75
Published on Web 09/12/2008

of the sol−gel process in situ via luminescent probes.[8] Furthermore, materials with organic dye species included in mesostructured silica have led to a number of advanced optical applications, such as optical switches and sensors,[9] and controlled drug-delivery systems.[10] Two general methods have been mainly developed for the production of such organically functionalized mesostructured materials. The first one is based on "postsynthetic grafting". Since the density of functional groups incorporated into the mesoporous channels is dependent on the density of the surface Si−OH groups, pore accessibility, and efficiency of the silylation reactions, this method suffers from many difficulties inherent in the preparation, for example, a quite low loading and an inhomogeneous distribution of the organic groups in the mesoporous materials, which are often located at the vicinity of the pore opening. The alternative method to synthesize organically functionalized mesoporous silica phases is the cocondensation method (one-pot synthesis). This approach involves cocondensation of silicate species and organosilicates that contain nonhydrolyzable functional ligands in the presence of templating surfactant molecules. During the coassembly process, organosilicates that contain hydrophobic ligands may serve as cosurfactants and insert the ligands into the hydrophobic micellar cores, resulting in a more homogeneous ligand distribution along the silicate/surfactant interface. However, the cocondensation method also has a number of disadvantages.[11] In general, the degree of mesoscopic order of the products decreases with increasing concentration of organic functionalities in the reaction mixture, which ultimately leads to mesostructure collapse.[5d]

Most recently, self-assembly of amphiphilic molecules that can serve as both structure-directing agents and monomers seems to be one promising approach used for the production of mesostructured nanocomposites.[12−15] Brinker and coworkers explored in situ polymerization using an amphiphilic diacetylenic surfactant as the structure-directing agent to template the formation of silica-type inorganic materials. The resulting polydiacetylene−silica composites are optically transparent and mechanically robust. They exhibit interesting thermo-, solvato-, and mechanochromatic properties.[12] Followed this pioneering work, the method has so far mainly been applied in inclusion of conjugated polymer chains in mesoporous channels. For example, surfactants containing pyrrole[14] or thiophene[15] have been recently synthesized and used as templates to prepare mesostructured polymer−silica nanocomposites. However, the functional surfactant (optically active) directed synthesis of organic−inorganic architectures that have structural features spanning from the nanometer to the micrometer scale and that exhibit novel optical functionalities is less explored. Here we develop the utility of the hybrid organic−inorganic self-assembly approach in driving the optically active functionalities within the periodical nanoscale silica channels and report a novel mesoscopically ordered pH-responsive nanocomposite. Two cationic ammonium surfactants that have special functional chromophoric groups at the ends of their hydrophobic tails are designed and synthesized and then used as both structure-directing agents and functional nano building blocks. The self-assembly process locks both organic and inorganic precursors into three-dimensional arrangements. In contrast with postsynthetic grafting techniques and the cocondensation method, the symmetry of the self-assembly architecture demonstrated here not only guarantees a dense filling and total homogeneous distribution of organic functionalities but also allows for the uniform and molecular level controllable incorporation of organic functional composites within a mesoscopically ordered inorganic environment (Scheme 1).

Controlled synthesis and properties of materials in response to chemical stimuli is a hallmark of biology. Employing such a process in nanoscale science and engineering can result in novel materials that rival or even exceed the structure and function of naturally occurring materials. In recent years, interest in stimulus-responsive materials has rapidly grown as a result of many potential applications such as in environmental monitoring, medical imaging and diagnostics, nanoelectronics, photonics, and computing.[2,16] With recent advances in mesostructured materials and nanotechnologies, the organization of stimulus-responsive organic composites in synergistic mesostructures through postsynthetic grafting or the cocondensation method have attracted significant interest with respect to such applications.[5,9,10] Nowadays,

(7) (a) Hernandez, R.; Franville, A. C.; Minoofar, P.; Dunn, B.; Zink, J. I. *J. Am. Chem. Soc.* **2001**, *123*, 1248. (b) Minoofar, P. N.; Hernandez, R.; Chia, S.; Dunn, B.; Zink, J. I.; Franville, A. C. *J. Am. Chem. Soc.* **2002**, *124*, 14388. (c) Minoofar, P. N.; Dunn, B.; Zink, J. I. *J. Am. Chem. Soc.* **2005**, *127*, 2656. (d) Johansson, E.; Zink, J. I. *J. Am. Chem. Soc.* **2007**, *129*, 14437.
(8) Keeling-Tucker, T.; Brennan, J. D. *Chem. Mater.* **2001**, *13*, 3331.
(9) (a) Fan, H.; Lu, Y.; Stump, A.; Reed, S. T.; Baer, T.; Schunk, R.; Perez-Luna, V.; López, G. P.; Brinker, C. J. *Nature* **2000**, *405*, 56. (b) Wirnsberger, G.; Scott, B. J.; Stucky, G. D. *Chem. Commun.* **2001**, 119. (c) Radu, D.; Lai, C.; Wiench, J.; Pruski, M.; Lin, V. *J. Am. Chem. Soc.* **2004**, *126*, 1640. (d) Descalzo, A.; Rurack, K.; Weisshoff, H.; Martínez-Máñez, R.; Marcos, M.; Amorós, P.; Hoffmann, K.; Soto, J. *J. Am. Chem. Soc.* **2005**, *127*, 184. (e) Wirnsberger, G.; Scott, B. J.; Chmelka, B. F.; Stucky, G. D. *Adv. Mater.* **2000**, *12*, 1450. (f) Descalzo, A. B.; Jimenez, D.; Marcos, M. D.; Martínez-Máñez, R.; Soto, J.; El Haskouri, J.; Guillém, C.; Beltrán, D.; Amorós, P.; Borrachero, M. V. *Adv. Mater.* **2002**, *14*, 966. (g) Liu, N.; Chen, Z.; Dunphy, D. R.; Jiang, Y.; Assink, R. A.; Brinker, C. J. *Angew. Chem., Int. Ed.* **2003**, *42*, 1731. (h) Liu, N.; Dunphy, D. R.; Atanassov, P.; Bunge, S. D.; Chen, Z.; López, G. P.; Boyle, T. J.; Brinker, C. J. *Nano Lett.* **2004**, *4*, 551.
(10) (a) Mal, N. K.; Fujiwara, M.; Tanaka, Y. *Nature* **2003**, *421*, 350. (b) Mal, N. K.; Fujiwara, M.; Tanaka, Y.; Taguchi, T.; Matsukata, M. *Chem. Mater.* **2003**, *15*, 3385. (c) Han, Y.-J.; Stucky, G. D.; Butler, A. *J. Am. Chem. Soc.* **1999**, *121*, 9897. (d) Hernandez, R.; Tseng, H.-R.; Wong, J. W.; Stoddart, J. F.; Zink, J. I. *J. Am. Chem. Soc.* **2004**, *126*, 3370. (e) Hernandez, R.; Tseng, H.-R.; Wong, J. W.; Stoddart, J. F.; Zink, J. I. *J. Am. Chem. Soc.* **2004**, *126*, 3370. (f) Leung, K. C.-F.; Nguyen, T. D.; Stoddart, J. F.; Zink, J. I. *Chem. Mater.* **2006**, *18*, 5919. (g) Zhu, Y.; Fujiwara, M. *Angew. Chem., Int. Ed.* **2007**, *46*, 2241. (h) Vallet-Regi, M.; Balas, F.; Arcos, D. *Angew. Chem., Int. Ed.* **2007**, *46*, 2.
(11) Angloher, S.; Kecht, J.; Bein, T. *Chem. Mater.* **2007**, *19*, 3568.
(12) (a) Lu, Y. F.; Yang, Y.; Sellinger, A.; Lu, M. C.; Huang, J. M.; Fan, H. Y.; Haddad, R.; Lopez, G.; Burns, A. R.; Sasaki, D. Y.; Shelnutt, J.; Brinker, C. J. *Nature* **2001**, *410*, 913. (b) Yang, Y.; Lu, Y. F.; Lu, M. C.; Huang, J. M.; Haddad, R.; Xomeritakis, G.; Liu, N. G.; Malanoski, A. P.; Sturmayr, D.; Fan, H. Y.; Sasaki, D. Y.; Assink, R. A.; Shelnutt, J. A.; van Swol, F.; Lopez, G. P.; Burns, A. R.; Brinker, C. J. *J. Am. Chem. Soc.* **2003**, *125*, 1269. (c) Peng, H. S.; Tang, J.; Pang, J. B.; Chen, D. Y.; Yang, L.; Ashbaugh, H. S.; Brinker, C. J.; Yang, Z. Z.; Lu, Y. F. *J. Am. Chem. Soc.* **2005**, *127*, 12782.
(13) Aida, T.; Tajima, K. *Angew. Chem., Int. Ed.* **2001**, *40*, 3803.
(14) Ikegame, M.; Tajima, K.; Aida, T. *Angew. Chem., Int. Ed.* **2003**, *42*, 2154.
(15) Yang, Z.; Kou, X.; Ni, W.; Sun, Z.; Li, L.; Wang, J. *Chem. Mater.* **2007**, *19*, 6222.

Scheme 1. Formation of the Nanocomposites with Molecular-Scale and Mesoscale Periodicities and the Representation of the External (pH) Stimulus-Responsive Process

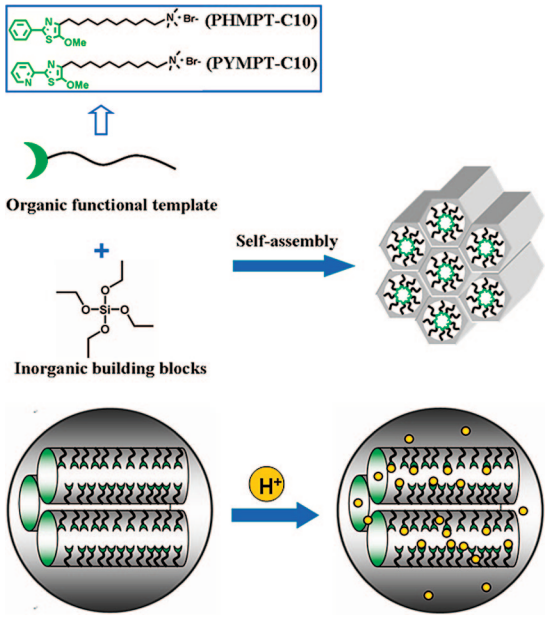

however, it is still a challenge to achieve better control of the organization mechanisms to prepare efficient complex structures while maintaining the organic moieties' integrity and accessibility, and thus hybrid architectures hierarchically organized in terms of structure and function. Herein, the hierarchical material design endows the obtained micrometer-sized mesostructured materials with strong fluorescence and recyclable pH-responsive properties and a rapid signal response. Furthermore, the rigid inorganic frameworks serve to enhance the mechanical, chemical, and thermal stability of the functional moieties, thus fostering their integration toward devices (Scheme 1). Such fluorescent mesostructured materials for pH detection in aqueous media can be of particular use, including medical, biological, and environmental applications.[17]

Experimental Section

Materials. All chemicals were of reagent grade and were used without further purification unless otherwise noted. 1,10-Dibromodecane, trimethylamine (32 wt % in ethanol), and *n*-butyllithium (BuLi) were purchased from Aldrich and Sigma-Aldrich. Tetraethyl orthosilicate (TEOS) and ammonia (25 wt %) were obtained from Beijing Chemical Reagent Co.

4-(10-Bromodecyl)-5-methoxy-2-phenylthiazole and 4-(10-Bromodecyl)-5-methoxy-2-pyridylthiazole. BuLi (1.6 M in hexane, 2.0 mmol) was added to a solution of 4-bromo-5-methoxy-2-phenylthiazole or 4-bromo-5-methoxy-2-pyridylthiazole (2.0 mmol) in dry THF (15 mL) at −78 °C. After the mixture was stirred at −78 °C for 30 min, 1,10-dibromodecane (12.0 mmol) dissolved in 5 mL of dry THF was added at once. The mixture was warmed to room temperature slowly and stirred overnight under an Ar atmosphere. The reaction was quenched by addition of water and then extracted with ethyl acetate. The organic layer was dried with anhydrous Na_2SO_4 and concentrated under reduced pressure. The residue was purified by column chromatography (ethyl acetate/petroleum ether, 20:1) to afford 4-(10-Bromodecyl)-5-methoxy-2-phenylthiazole or 4-(10-Bromodecyl)-5-methoxy-2-pyridylthiazole as a light yellow oil. The following are data for 4-(10-bromodecyl)-5-methoxy-2-phenylthiazole. ^{1}H NMR ($CDCl_3$): δ = 7.82−7.84 (m, 2 H), 7.35−7.41 (m, 3 H), 3.94 (s, 3 H), 3.38−3.42 (t, 2 H), 2.66−2.70 (t, 2 H), 1.81−1.88 (m, 2 H), 1.66−1.71 (m, 2 H), 1.28−1.41 (m, 12 H) ppm. MS (EI): m/z = 410 [M^+]. The following are data for 4-(10-bromodecyl)-5-methoxy-2-pyridylthiazole. ^{1}H NMR ($CDCl_3$): δ = 8.51−8.53 (d, 1 H), 8.06−8.07 (d, 1 H), 7.70−7.75 (t, 1 H), 7.20−7.24 (t, 1 H), 3.97 (s, 3 H), 3.38−3.42 (t, 2 H), 2.65−2.70 (t, 2 H), 1.81−1.88 (m, 2 H), 1.65−1.73 (m, 2 H), 1.29−1.43 (m, 12 H) ppm. MS (EI): m/z = 412 [M^+].

Trimethyl(10-(5-methoxy-2-phenylthiazol-4-yl)decyl)ammonium Bromide (PHMPT-C10) and Trimethyl(10-(5-methoxy-2-pyridylthiazol-4-yl)decyl)ammonium Bromide (PYMPT-C10). PHMPT-C10 and PYMPT-C10 were prepared as follows: The bromine-terminated compound 4-(10-bromodecyl)-5-methoxy-2-phenylthiazole or 4-(10-bromodecyl)-5-methoxy-2-pyridylthiazole (0.5 mmol) was added to a trimethylamine solution in ethanol (10 mL, 32 wt %). The flask was sealed, allowed to stand at room temperature for 1 day, and then heated at 55 °C for 2 days. After being cooled to room temperature, the mixture was concentrated under reduced pressure, and the white solid product was collected, washed with dry THF, and dried in a vacuum. The following are data for PYMPT-C10. ^{1}H NMR ($CDCl_3$): δ = 7.80−7.82 (m, 2 H), 7.28−7.40 (m, 3 H), 3.93 (s, 3 H), 3.53−3.57 (t, 2 H), 3.46 (s, 9 H), 2.64−2.68 (t, 2 H), 1.66−1.72 (m, 4 H), 1.25−1.34 (m, 12 H) ppm. MS (ESI): m/z = 388 [M^+]. The following are data for PYMPT-C10. ^{1}H NMR ($CDCl_3$): δ = 8.51−8.53 (d, 1 H), 8.04−8.07 (d, 1 H), 7.71−7.75 (t, 1 H), 7.21−7.24 (t, 1 H), 3.97 (s, 3 H), 3.54−3.58 (t, 2 H), 3.47 (s, 9 H), 2.65−2.69 (t, 2 H), 1.66−1.72 (m, 4 H), 1.28−1.34 (m, 12 H) ppm. MS (ESI): m/z = 390 [M^+].

Synthesis of Mesostructured PHMPT-C10−Silica and PYMPT-C10−Silica Nanocomposite Particles. The mesostructured nanocomposites were synthesized as follows: A 0.57 mmol sample of functional template (PHMPT-C10 or PYMPT-C10) was dissolved in 10 mL of H_2O and 4.8 g of concentrated NH_3 (25%) under stirring, and 1 g of TEOS was added dropwise to the solution. The mixture was stirred for 30 min at room temperature, and then the temperature was elevated to 90 °C and kept at 90 °C for another 5 h in a Teflon-lined autoclave. Finally, the resulting precipitate was filtered and washed thoroughly with distilled water. The sample was dried in a vacuum at room temperature. Elemental analysis: (nanocomposites made from PHMPT-C10) C, 27.69; H, 4.47; N, 2.68; (nanocomposites made from PYMPT-C10) C, 24.19; H, 4.21; N, 3.57.

Characterization. ^{1}H NMR spectra were recorded on a Bruker ARX 400 spectrometer with trimethylsilane (TMS) as the internal standard. X-ray powder diffraction (XRD) patterns of the nanocomposite particles were recorded on a Rigaku Dmax-2000 X-ray powder diffractometer (Japan) using Cu Kα (λ = 1.5405 Å) radiation. Scanning electron microscopy (SEM) observations were carried out with a DB-235 focused ion beam (FIB) system operated

(16) (a) Li, D.; Sheng, X.; Zhao, B. *J. Am. Chem. Soc.* **2005**, *127*, 6248. (b) Miyawaki, A.; Llopis, J.; Helm, R.; McCaffery, J. M.; Adams, J. A.; Ikura, M.; Tsien, R. Y. *Nature* **1997**, *388*, 882. (c) Turner, F. *Science* **2000**, *290*, 1315. (d) Rottman, C.; Grader, G.; De Hazan, Y.; Melchior, S.; Avnir, D. *J. Am. Chem. Soc.* **1999**, *121*, 8533. (e) Lim, H. S.; Han, J. T.; Kwak, D.; Jin, M.; Cho, K *J. Am. Chem. Soc.* **2006**, *128*, 14458. (f) Lee, M.; Lee, S.; Jiang, L. H. *J. Am. Chem. Soc.* **2004**, *126*, 12724. (g) Liu, J.; Lu, Y. *J. Am. Chem. Soc.* **2005**, *127*, 12677. (h) Lu, Y.; Liu, J. *Acc. Chem. Res.* **2007**, *40*, 315.
(17) Sun, H.; Scharff-Poulsen, A. M.; Gu, H.; Almdal, K. *Chem. Mater.* **2006**, *18*, 3381.

Scheme 2. Synthetic Procedures of the Functional Chromophoric Group Containing Cationic Surfactants PHMPT-C10 and PYMPT-C10

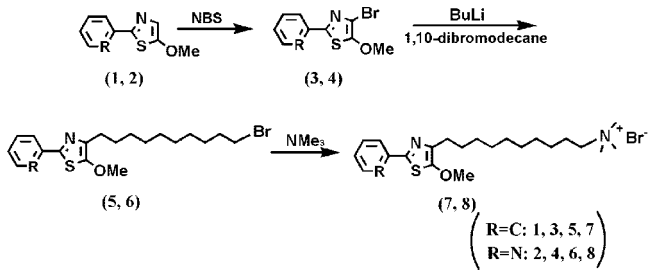

at an acceleration voltage of 15 kV. TEM images were taken on a Hitachi H-9000 NAR transmission electron microscope under a working voltage of 300 kV. The nitrogen adsorption and desorption isotherms were measured using an ASAP 2010 analyzer (Micromeritics Co. Ltd.) at 78.3 K, and pore size distributions were calculated using the Barret−Joyner−Halenda (BJH) model on the adsorption branch. Elemental analyses (C, H, N) were performed on an Elementar Vario EL analyzer. Weight changes of the products were carried out on a Thermal Analysis SDT Q600 analyzer (America) from 100 to 800 °C under air with a heating rate of 10 °C/min. IR spectra were recorded on a Nicolet Magna-IR 750 spectrometer equipped with a Nic-Plan microscope. Cross-polarization ^{13}C MAS NMR spectra were recorded on a Varian-Unity INOVA 300 MHz spectrometer operating at 75.476 MHz (2.55 μs pulse widths, 10 000 transients, spinning speed of 5 kHz, contact time 4 s, pulse delay 5 s). Diffuse reflectance (DR) UV/vis spectra were recorded on a Shimadzu UV-3100 spectrometer equipped with a diffuse reflectance accessory and using $BaSO_4$ as a reference. The fluorescence spectra were recorded on a Hitachi F-4500 fluorescence spectrophotometer.

Results and Discussion

The methodology for synthesis of the two functional chromophoric group containing cationic surfactants PHMPT-C10 and PYMPT-C10 is summarized in Scheme 2. The two functional chromophoric groups, 5-methoxy-2-phenylthiazole (**1**, PHMPT) and 5-methoxy-2-pyridylthiazole (**3**, PYMPT), were synthesized according to the literature.[18,19] Subsequent bromination of the 4-position with NBS led to 4-bromo-5-methoxy-2-phenylthiazole (**2**) and 4-bromo-5-methoxy-2-pyridylthiazole (**4**).[18,19b] 4-(10-Bromodecyl)-5-methoxy-2-phenylthiazole (**5**) and 4-(10-bromodecyl)-5-methoxy-2-pyridylthiazole (**6**) were then synthesized by treating **2** and **4** with *n*-BuLi in THF and quenching the 4-lithio-5-methoxy-2-phenylthiazole and 4-lithio-5-methoxy-2-pyridylthiazole with 1,10-dibromodecane. The cationic ammonium surfactants PHMPT-C10 and PYMPT-C10 (**7** and **8**, respectively), which have different functional chromophoric groups at the ends of their hydrophobic tails, were then obtained by the reaction of trimethylamine with the bromodecyl-terminated **5** and **6** in alcoholic solutions.

The special chromophoric group containing surfactants PHMPT-C10 and PYMPT-C10 were used as structure-directing agents to prepare mesostructured composite particles in a one-phase route under strongly basic conditions,[20] as shown schematically in Scheme 1. TEOS was used as the silica precursor. During reaction, particles were observed to form and precipitate to the bottom of the container. These particles were washed and deposited onto silicon substrates for SEM observation. It shows that the materials prepared with PHMPT-C10 are micrometer-sized particles without a precise structure. In contrast, the nanocomposites from PYMPT-C10 are formed as silica spheres with diameters of about 500 nm (Figure 1). The quantities of amphiphilic functional molecules within the mesostructures (L_0 = 0.93 and 0.85 mmol·g^{-1} for nanocomposites obtained from PHMPT-C10 and PYMPT-C10, respectively) were calculated from the percentage of nitrogen in the nanocomposites, as estimated by elemental analysis. Thermogravimetric analysis (TGA) of the nanocomposites (see Figure S1 in the Supporting Information) reveals contents of the functional organic monomer of 42 and 40 wt %, respectively, which are as high as those reported for conventional mesoporous silicates containing template surfactants.[3] The amount of organic moieties calculated from this weight loss is comparable with that estimated from the elemental analysis of nitrogen.

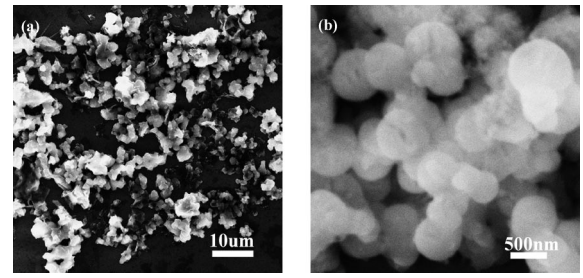

Figure 1. SEM images of the mesostructured nanocomposites formed from (a) PHMPT-C10 and (b) PYMPT-C10.

The IR and ^{13}C MAS NMR spectra were measured to characterize the chemical structure of these composite materials, respectively. Figure 2 shows the IR spectra of the functional surfactants and the resultant nanocomposites between 4000 and 600 cm^{-1}. Both the nanocomposites presented characteristic bands for aliphatic C−H stretching vibrations of alkyl chains around 2950−2820 cm^{-1} and a strong band centered at 1080 cm^{-1} due to the stretching vibrations of the Si−O−Si framework. The bands at ca. 1480 and 1550 cm^{-1} were assigned to C═C and C═N stretching vibrations of the PHMPT and PYMPT functional groups. ^{13}C MAS NMR spectra along with the peak assignments are given in Figure 3 for the functional surfactants and the resultant nanocomposites. The carbons directly bonded to the nitrogen of the functional surfactants exhibit a slight low-field shift (from 51.8 to 53.5 ppm for C1−C3, from 64.3 to 66.7 ppm for C4) when the chromophore−silica composites are formed, which is characteristic of a restricted mobility of the surfactant head due to the electrostatic binding between the electropositive group of the surfactant and the silicate

(18) Takami, S.; Kawai, T.; Irie, M. *Eur. J. Org. Chem.* **2002**, 3796.
(19) (a) Zheng, M. H.; Jin, J. Y.; Sun, W.; Yan, C. H. *New J. Chem.* **2006**, *30*, 1192. (b) Li, L. L.; Sun, H.; Fang, C. J.; Xu, J.; Jin, J. Y.; Yan, C. H. *J. Mater. Chem.* **2007**, *17*, 4492.
(20) Asefa, T.; MacLachlan, M. J.; Coombs, N.; Ozin, G. A. *Nature* **1999**, *402*, 867.

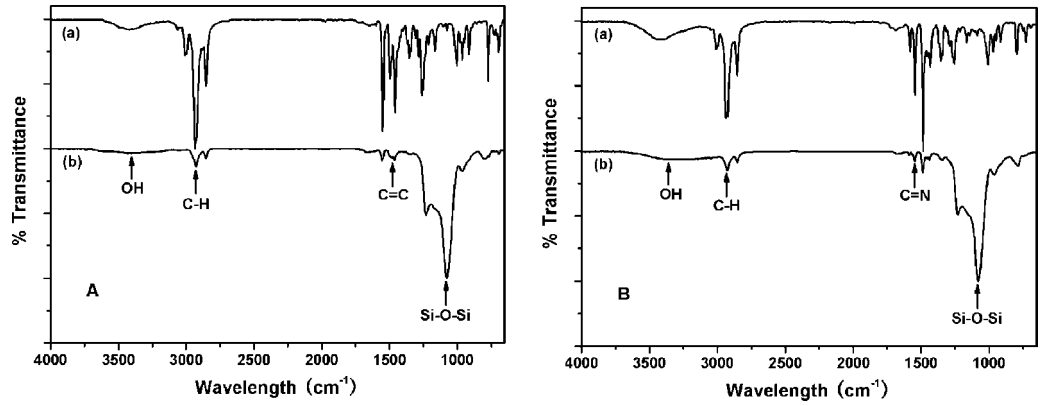

Figure 2. FT-IR spectra of (A) (a) PHMPT-C10 and (b) nanocomposites formed from PHMPT-C10 and (B) (a) PYMPT-C10 and (b) nanocomposites from PYMPT-C10.

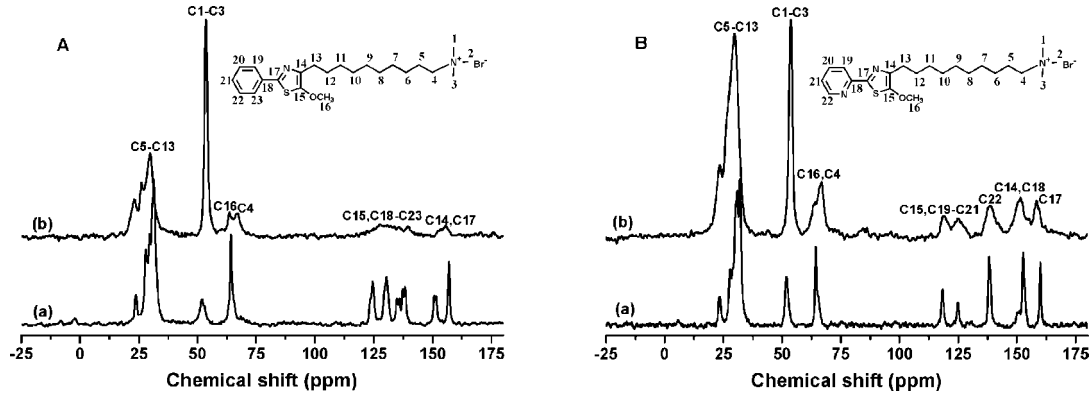

Figure 3. ^{13}C MAS NMR spectra of (A) (a) PHMPT-C10 and (b) nanocomposites formed from PHMPT-C10 and (B) (a) PYMPT-C10 and (b) nanocomposites from PYMPT-C10.

substrate.[21,22] The remainder of the internal methylenes (C5−13) are lumped together in the broad peak centered at 39.5 ppm. The peaks at higher chemical shifts between 120 and 160 ppm are assigned to the conjugated carbon atoms of the incorporated PHMPT and PYMPT functional groups. The lower signal-to-noise ratio at higher chemical shifts for the PHMPT-C10 nanocomposites is characteristic of a decrease of surfactant mobility, due to a more confined space of the ordered mesostructure.[22,23]

Figure 4 shows the powder XRD pattern of the resultant nanocomposites. The nanocomposites obtained with PHMPT-C10 are proven to be a typical two-dimensional hexagonal *p6mm* mesophase (Figure 4a). The three well-resolved peaks are indexed to (100), (110), and (200) diffractions of a hexagonal structure and correspond to a d_{100} distance of 3.84 nm. The XRD pattern (Figure 4b) of the sample derived from PYMPT-C10 shows only a broad and intense single Bragg peak around $2\theta = 2.8°$, characteristic of periodic mesoscopic silicate structures and corresponding to a d spacing for the (100) diffraction peak of 3.15 nm. The absence of other diffraction peaks suggests that the mesostructure of the particles prepared with PYMPT-C10 is less ordered than that derived from PHMPT-C10. TEM

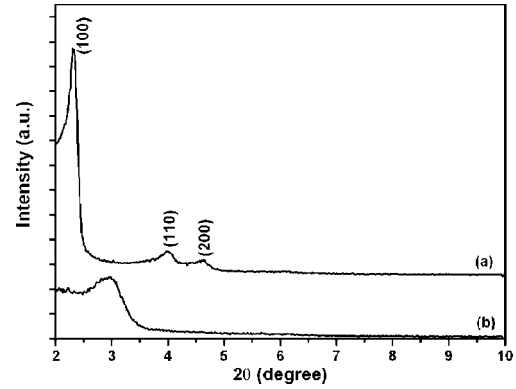

Figure 4. XRD patterns of the mesostructured nanocomposites formed from (a) PHMPT-C10 and (b) PYMPT-C10.

images (Figure 5) of the nanocomposites reveal that the composite with PYMPT-C10 has a uniform mesostructure but with only short-range ordering,[24] whereas the nanocomposite produced with PHMPT-C10 displays hexagonally arranged mesopores throughout the sample with a center to center distance between the hexagon centers of 3.6−4.0 nm, which is comparable with the XRD results.

It was demonstrated that the surfactant packing, which is the dominant factor in determining the final structure of the

(21) Simonutti, R.; Comotti, A.; Bracco, S.; Sozzani, P. *Chem. Mater.* **2001**, *13*, 771.
(22) Wang, L. Q.; Liu, J.; Exarhos, G. J.; Bunker, B. C. *Langmuir* **1996**, *12*, 2663.
(23) Petitto, C.; Galarneau, A.; Driole, M. F.; Chiche, B.; Alonso, B.; Renzo, F. D.; Fajula, F. *Chem. Mater.* **2005**, *17*, 2120.
(24) (a) Bagshaw, S. A.; Prouzet, E.; Pinnavaia, T. J. *Science* **1995**, *269*, 1242. (b) Prouzet, E.; Cot, F.; Nabias, G.; Larbot, A.; Kooyman, P.; Pinnavaia, T. J. *Chem. Mater.* **1999**, *11*, 1498.

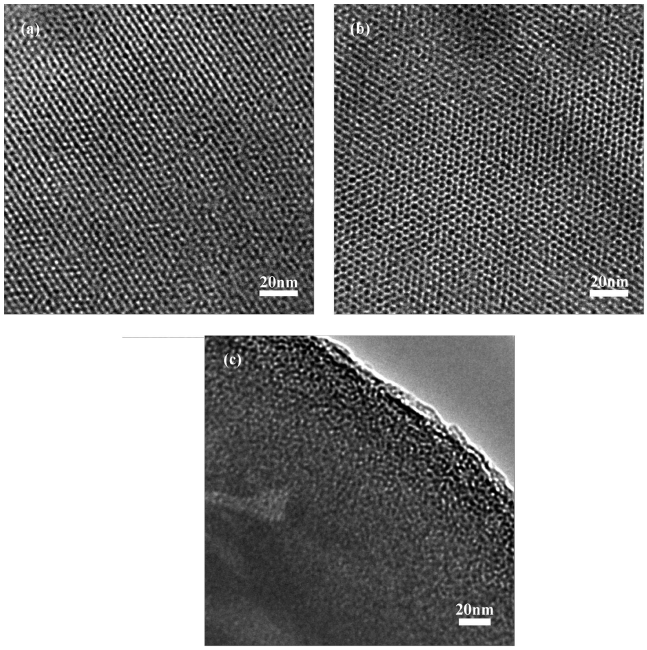

Figure 5. TEM images of the nanocomposites from PHMPT-C10 recorded in the direction perpendicular to the pore axis (a) and in the direction of the pore axis (b) and of the nanocomposite from PYMPT-C10 (c).

mesoporous materials,[25] depends on the molecular geometry of the surfactants, such as the number of carbon atoms in the hydrophobic chain,[25a] the size or charge of the polar headgroup,[26] and the molecular shape.[27] The functional templates PHMPT-C10 and PYMPT-C10, which are amphiphiles that have a single alkyl chain with a chromophore (PHMPT or PYMPT) as the hydrophobic part and a trimethylammonium headgroup as the hydrophilic part, have almost the same molecular size and shape. Thus, it is reasonable to deduce that the different mesostructures exhibited by the products synthesized with the two functional surfactants result from the intrinsic properties (specifically, the hydrophobic property) of the chromophore groups (PHMPT and PYMPT) attached at the tail ends of the surfactants. In comparison with the hydrophobic chromophoric group PHMPT, PYMPT exhibits a better hydrophilic property (solubility in water 0.001 and 0.05 mg mL^{-1} for PHMPT and PYMPT, respectively), which would decrease the effective surfactant hydrophobic tail area of PYMPT-C10 and thus perturb the assembly and topology of amphiphile surfactants and consequently the mesostructures of the resulting nanocomposites.[25] This is in agreement with the observation from the XRD and TEM characterizations that the PYMPT-C10-directed mesostructure is less ordered than the PHMPT-C10-directed one. In addition, the *d* spacing of the PYMPT-C10-directed particles is smaller

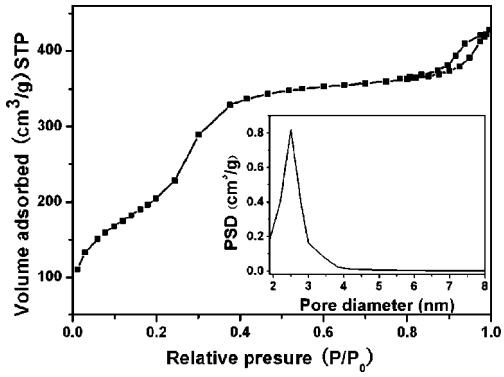

Figure 6. Nitrogen adsorption−desorption isotherms of the calcined nanocomposite formed from PHMPT-C10. Inset: corresponding pore size distribution for the calcined samples.

than that of the PHMPT-C10-directed particles, which also can be attributed to the decrease in the degree of the effective hydrophobic tail area of the PYMPT-C10 and a less ordered mesostructure directed by this surfactant. The better ordering observed in the PHMPT-C10-directed mesostructure is essentially due to the larger hydrophobic interaction between the longer effective tails, as supported by the previous estimation that the standard free energy of micellization becomes more negative as the hydrophobic tail of the alkyltrimethylammonium bromide surfactant gets longer.[15,28]

The mesostructure of the nanocomposites was also confirmed by the calcination of the hybrids at 550 °C for 5 h to remove the organic components. The XRD patterns of the calcined samples show that the mesostructure with short-range ordering (PYMPT-C10) collapsed upon calcination, while the highly ordered inorganic framework was retained in the case of the calcined PHMPT-C10 hybrid, although the *d* spacing had decreased to 37.7 Å. The N_2 sorption isotherm of the resulting mesoporous silica is shown in Figure 6. It is of type IV and exhibits a minor amount of hysteresis. The inset figure shows a quite narrow pore size distribution calculated from the adsorption isotherm. The pore diameter, 2.5 nm, is smaller than that of the nanocomposites deduced from TEM and XRD results due to shrinkage during calcination.[12b]

DR UV/vis spectra and fluorescence spectra were measured to characterize the optical properties of both the mesostructured chromophore−silica composite particles. The absorption bands of PHMPT-C10 and PYMPT-C10 surfactants in the solid state are observed at 352 and 370 nm, but when chromophore−silica composites are formed, their maximum absorption undergoes a blue shift of about 20 and 12 nm, respectively (Figure 7a,b). Figure 7c,d shows the fluorescence spectra of the two composite particle samples. The PHMPT-C10−silica and PYMPT-C10−silica composite particles exhibit fluorescence peaks centered around 400 and 425 nm, respectively. It is clearly seen that both the fluorescence maxima of the nanocomposites also exhibit an obvious blue shift (8 and 20 nm, respectively) in comparison with those of the two functional surfactants. The possible reason for the absorption or fluorescence shift is that the functional surfactant molecules are nanoscopically packed

(25) (a) Tolbert, S. H.; Landry, C. C.; Stucky, G. D.; Chmelka, B. F.; Norby, P.; Handon, J. C.; Monnier, A. *Chem. Mater.* **2001**, *13*, 2256. (b) Monnier, A.; Schüth, F.; Huo, Q.; Kumar, D.; Margolese, D.; Maxwell, R. S.; Stucky, G. D.; Krishnamurty, M.; Petroff, P.; Firouzi, A.; Janicke, M.; Chmelka, B. F. *Science* **1993**, *261*, 1303.

(26) Huo, Q.; Margolese, D. I.; Ciesla, U.; Demuth, D. G.; Feng, P.; Gier, T. E.; Sieger, P.; Firouzi, A.; Chmelka, B. F.; Schüth, F.; Stucky, G. D. *Chem. Mater.* **1994**, *6*, 1176.

(27) (a) Bhongale, C. J.; Hsu, C.-S. *Angew. Chem., Int. Ed.* **2006**, *45*, 1404. (b) Shen, S.; Garcia-Bennett, A. E.; Liu, Z.; Lu, Q.; Shi, Y.; Yan, Y.; Yu, C.; Liu, W.; Cai, Y.; Terasaki, O.; Zhao, D. *J. Am. Chem. Soc.* **2005**, *127*, 6780.

(28) Gao, J. X.; Bender, C. M.; Murphy, C. J. *Langmuir* **2003**, *19*, 9065.

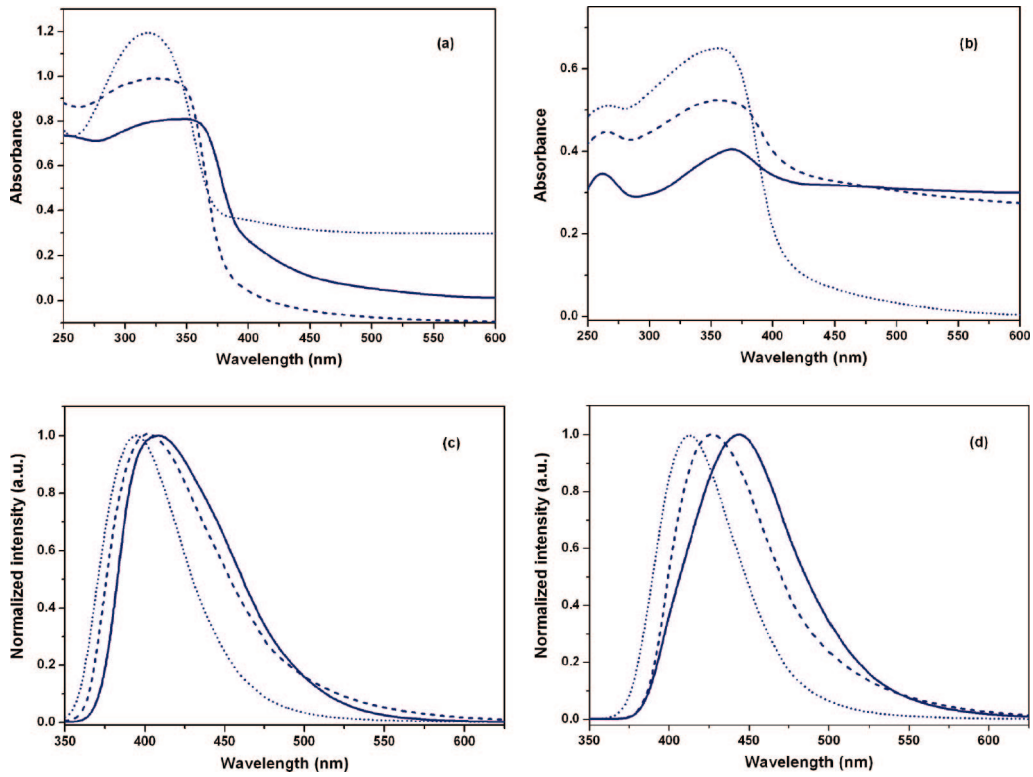

Figure 7. Optical properties of the mesostructured composite particles. Diffuse reflectance UV/vis spectra of (a) PHMPT-C10 (solid lines), nanocomposites formed from PHMPT-C10 (dashed lines), and the composite $\mathbf{2}_{\text{PHMPT-C10/CTAB}}$ directed by CTAB and PHMPT-C10 (dotted lines) and (b) PYMPT-C10 (solid lines), nanocomposites from PYMPT-C10 (dashed lines), and the composite $\mathbf{2}_{\text{PYMPT-C10/CTAB}}$ directed by CTAB and PYMPT-C10 (dotted lines). Fluorescence emission spectra of (c) PHMPT-C10 (solid lines), nanocomposites formed from PHMPT-C10 (dashed lines), and the composite $\mathbf{2}_{\text{PHMPT-C10/CTAB}}$ (dotted lines) and (d) PYMPT-C10 (solid lines), nanocomposites from PYMPT-C10 (dashed lines), and the composite $\mathbf{2}_{\text{PYMPT-C10/CTAB}}$ (dotted lines).

and separated by inorganic channels.[27a,29,30] Meanwhile, the environment of the silicate channels may also be a factor in the optical change of the composites, as the previous reports showed that the local environment (such as pH) of the matrix can affect the fluorescence shift of the dyes.[31] We are motivated to disclose the effects of this nanoscopic segregation on the optical properties of the guest chromophores. PHMPT-C10 or PYMPT-C10 was diluted with a conventional ammonium surfactant (cetyl trimethylammonium bromide, CTAB) at a molar ratio of [PHMPT-C10 or PYMPT-C10]:[CTAB] = 1:9, and the mixtures were utilized as co-structure-directing agents for the sol−gel process. Since the length of PHMPT-C10 or PYMPT-C10 is similar to that of a CTAB molecule, the functional templates should pack efficiently into micelles with CTAB, and its placement is an example of the "philicity" strategy.[7d,13,29] The obtained hybrids $\mathbf{2}_{\text{PHMPT-C10/CTAB}}$ and $\mathbf{2}_{\text{PYMPT-C10/CTAB}}$ showed XRD patterns characteristic of hexagonal structures with *d* spacings of 41.3 and 40.5 Å, respectively (Figure 8). This correlates well with the CTAB-only composite materials made by a similar procedure, which typically have center to center pore distances of 39−40 Å.[32] In comparison with the free

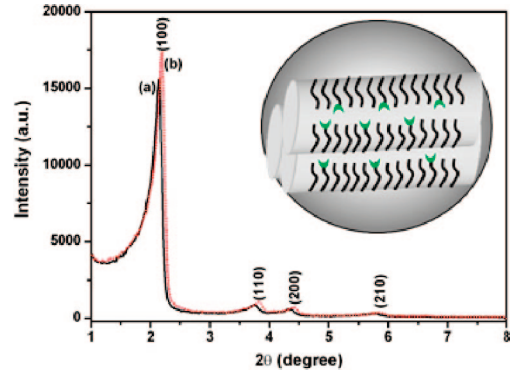

Figure 8. XRD patterns of the mesostructured composites (a) $\mathbf{2}_{\text{PHMPT-C10/CTAB}}$ and (b) $\mathbf{2}_{\text{PYMPT-C10/CTAB}}$. Inset: representation of the placement of the co-structure-directing agents in the obtained mesostructures.

functional surfactants PHMPT-C10 and PYMPT-C10, both the composites $\mathbf{2}_{\text{PHMPT-C10/CTAB}}$ and $\mathbf{2}_{\text{PYMPT-C10/CTAB}}$ demonstrate much higher blue shifts of absorption (32 and 17 nm, respectively) and fluorescence (16 and 35 nm, respectively). In the composite $\mathbf{2}_{\text{PHMPT-C10/CTAB}}$ or $\mathbf{2}_{\text{PYMPT-C10/CTAB}}$, the functional surfactants should be fairly well isolated (Figure 8, inset), because both there is only a small amount of functional surfactants relative to CTAB and electrostatic repulsion and packing frustration should again separate any chains that assemble into the same domain.[7d,29] Since the interaction of the chromophoric groups is smaller in the CTAB/functional surfactant codirected composites than that directed only by functional surfactants (PHMPT-C10 or PYMPT-C10), we conclude that such a blue shift in absorption and fluorescence between the free functional

(29) Clark, A. P.-Z.; Shen, K.; Rubin, Y. F.; Tolbert, S. H. *Nano Lett.* **2005**, *5*, 1647.
(30) Tsai, F. Y.; Tub, H.-L.; Mou, C.-Y. *J. Mater. Chem.* **2006**, *16*, 348.
(31) (a) Rottman, C.; Avnir, D. *J. Am. Chem. Soc.* **2001**, *123*, 5730. (b) Rottman, C.; Grader, G.; Hazan, Y. D.; Melchior, S.; Avnir, D. *J. Am. Chem. Soc.* **1999**, *121*, 8533.
(32) Firouzi, A.; Kumar, D.; Bull, L. M.; Besier, T.; Sieger, P.; Huo, Q.; Walker, S. A.; Zasadzinski, J. A.; Glinka, C.; Nicol, J.; Margolese, D.; Stucky, G. D.; Chmelka, B. F. *Science* **1995**, *267*, 1138.

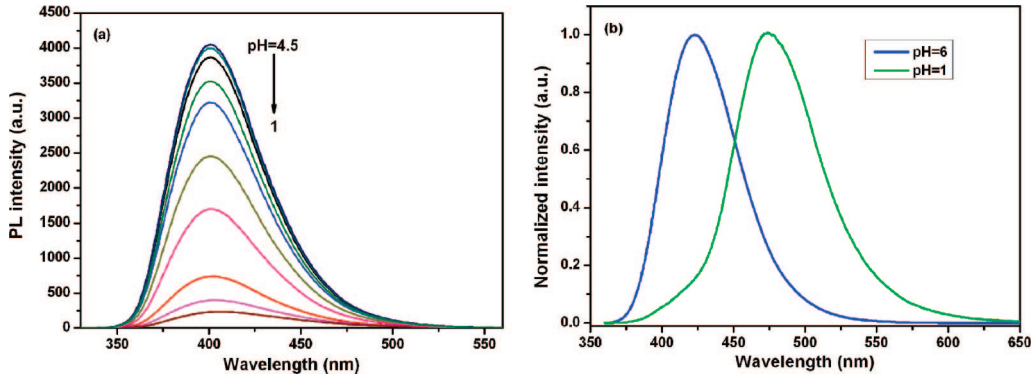

Figure 9. Evolutions of fluorescence emission of the mesostructured composite particles formed from (a) PHMPT-C10 and (b) PYMPT-C10 with pH (λ_{exc} = 315 and 350 nm, respectively).

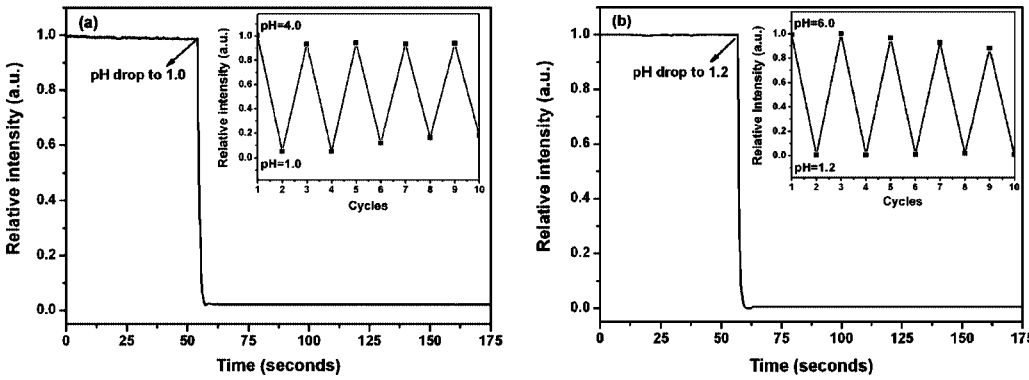

Figure 10. Time-dependent fluorescence response of the nanocomposites formed from (a) PHMPT-C10 and (b) PYMPT-C10 upon a change of the pH value. Inset: PL intensities of the nanocomposites during pH switching cycles. For the PHMPT-C10 nanocomposite, λ_{exc} = 315 nm and λ_{em} = 400 nm. For the PYMPT-C10 nanocomposite, λ_{exc} = 350 nm and λ_{em} = 420 nm.

surfactants and the composites is mainly attributable to the nanoscopic insulation of the fluorescent surfactant domain in composite materials by the silicate channels. A similar blue shift of the fluorescence of conjugated polymers has been observed in a confined space and under a rigid environment.[29] The present example also suggests that the interaction of the chromophoric groups and further the optical properties of the composites can be modulated by using conventional ammonium surfactants as co-structure-directing agents for tailoring the self-assembly progress.

The responsive properties of the mesostructured composite particles to external stimuli (pH) were demonstrated by subjecting the nanocomposites to aqueous solutions with different pH values. The emission intensity of the nanocomposite derived from PHMPT-C10 at ca. 400 nm was quenched monotonically with a slight blue shift with a decrease of the pH from 4.5 to 1, while the shape of the emission band remained constant in these spectra (Figure 9a). In contrast, the PYMPT-C10 nanocomposite displays a pH-sensitive ratiometric fluorescent behavior. The fluorescence spectrum of the nanocomposite shows a significant peak shift corresponding to the pH, from λ_{max} = 422 nm for pH 6 to λ_{max} = 475 nm for pH 1 (Figure 9b). The different responsive behaviors of the two nanocomposites are attributed to the special chromophoric groups (PHMPT and PYMPT) at the tails of the functional surfactants. It has been deduced that the internal charge transfer (ICT) process evolved upon excitation and photoinduced charge transfer occurring from the electron donor 5-methoxy group to the 2-phenyl ring (for PHMPT) or to the 2-pyridyl ring (for PYMPT).[19] The ICT process is well-known to be very sensitive to small perturbations that can induce spectroscopic changes and has been used a lot in the past for the synthesis of small molecular reporter compounds.[33] The bathochromic emission of PYMPT was assigned to the protonated form, PYMPT$-H^+$. Upon prior protonation of the pyridyl nitrogen atom, the energy gap between the highest occupied molecular orbital (HOMO) and the lowest unoccupied molecular orbital (LUMO) is decreased, which favors the ICT from the methoxy group to the pyridyl group through the thiazole ring and results in a bathochromic shift of fluorescence.[19] In contrast, the protonation of the chromophoric group PHMPT occurs at the nitrogen atom of the thiazole ring, which reduces the ICT character of the molecule and is responsible for the quenched fluorescence intensity.[33]

An important requirement to be considered in preparing a hybrid optically sensitive material is the short response time. Figure 10 shows the time-dependent fluorescence response of the two nanocomposites upon changing the pH. It is noted that both the response time are fast, in a few seconds, which is much faster than that of optical pH sensors based purely

(33) (a) Gunnlaugsson, T.; Leonard, J. P.; Murray, N. S. *Org. Lett.* **2004**, *6*, 1557. (b) Lu, C.; Xu, Z.; Cui, J.; Zhang, R.; Qian, X. *J. Org. Chem.* **2007**, *72*, 3554. (c) Charier, S.; Ruel, O.; Baudin, J.; Alcor, D.; Allemand, J.; Meglio, A.; Jullien, L. *Angew. Chem., Int. Ed.* **2004**, *43*, 4785.

on a sol−gel.[34] Such a rapid response to the external chemical stimuli is interesting, when the accessibility of functionalities inside the channels to the solution with protons is considered. A similar fast diffusion of the solution with small molecules toward the inorganic channels, which were filled with the surfactant templates, have also been observed in previous reports.[12a,b,14] Aida et al. have used the surfactant carrying a pyrrole group as the structure-directing agent to prepare mesostructured silica-based hybrid composites. It was demonstrated that the initiator ($FeCl_3$) solution can quickly (within 1 min) diffuse into the silica channels and polymerize the included pyrrole-containing surfactants.[14] Brinker et al. have also demonstrated that different polar solvent molecules could penetrate within the polydiacetylene-packed silica channels and induce a solvatochromic behavior, suggesting applications in sensing.[12a,b] Although a further detailed study of such accessibility is needed, the present example suggests that the unique mesotructure of the nanocomposites facilitates the fast diffusion and transport of small analytes. Furthermore, the reusability and reproducibility of the hybrid optical sensors are of particular interest in developing recyclable chemosensing materials, highlighting their desirability for industrial applications.[35] As is evident from the data in Figure 10 (inset), the optical switching of fluorescence can be achieved over 10 pH cycles without apparent "fatigue" effects. The fluorescent stimulus-responsive hybrid nanocomposite particles could therefore be of particular use in a number of applications, including tagging, tracing, and labeling.[2,36]

It is known that the cationic surfactants, which were entrapped in mesostructures through the electrostatic interaction between the electropositive group of the surfactant and the silicate substrate, can be washed out slowly when these materials come in contact with water.[37] Leaching of the functionalities from the nanocomposites during longer times was tested by preparing a 2.5 mg/mL suspension of the materials in buffer solution (2 mL, pH 4.0), transferring the suspension to a dialysis cassette, and immersing the cassette into a continuously stirred buffer solution (38 mL). The fluorescence emission from the solution outside the cassette was measured at appropriate time points to evaluate the leaching ratio.[17] The obtained results are shown in Figure 11. It is seen that the functional surfactants leached fast at the beginning. Within the first 7 h, a total of ca. 5% and 10% of the embedded functionalities had leached out of the two particles, respectively, whereas further leaching was extremely slow. It is interesting to note that the PYMPT-C10 composites exhibited a release activity superior to that derived from PHMPT-C10. According to the aforementioned XRD and TEM analyses, the pore morphologies of these

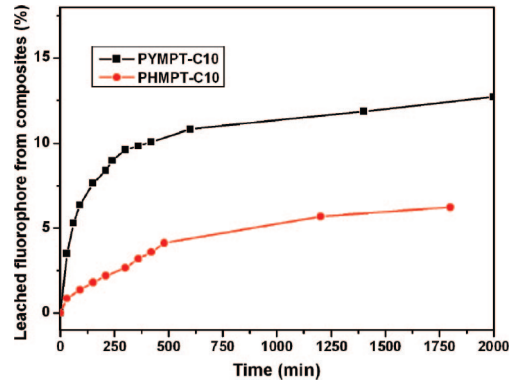

Figure 11. Leaching rate of the functionalities (a) PHMPT-C10 and (b) PYMPT-C10 out of the respective nanocomposites in aqueous buffer solution (pH 4.0).

two samples are very different. The PHMPT-C10 composite has hexagonal ordered pores, while the PYMPT-C10 composite has a disordered wormhole-like pore arrangement. The wormhole-like structure is best described as one-dimensional rod-type micelles entangled in a three-dimensional manner. As a result, this structure provides an isotropic porous structure with easily accessible pore openings from any direction.[38] It is plausible that the rate of functional surfactant release via diffusion from the isotropic disordered porous structure of the PYMPT-C10 composite would be faster than that of the ordered hexagonal channels of the PHMPT-C10 composite. This structure-dependent release activity of the one-pot assembled functional materials provides insight into the future design of drug delivery systems that can release drugs with different structural dimensions.[10]

Given the potential to use such nanostructured materials for biological sensing and controlled delivery systems, we set out to investigate the relative stability of such materials to their environment under biologically relevant conditions. The nanocomposites were exposed to aqueous environments at 37 °C consisting of cell culture media supplemented with 10% fetal bovine serum (FBS). It has been demonstrated by Sanchez et al.[39] that exposure to such media resulted in somewhat faster destruction of the silica mesostructure, which is probably a result of the presence of active nucleophiles in the culture media. XRD measurements were used to observe changes of the mesostructures as a function of the exposure time (see Figure S2 in the Supporting Information). Upon exposure, a steady decrease in the d_{100} spacing as well as a decrease in the intensity of the (100) peak can be observed for the composites obtained with PHMPT-C10. Nevertheless, the hexagonal structure still remains, even after exposure for 5 h. In contrast, for the nanocomposites derived from PYMPT-C10, exposure in such aqueous media has a marked effect on the textural properties. The intensity of the (100) peak in the XRD pattern of the composites exposed for 5 h has decreased markedly and is almost undetectable, which indicates that the mesostructure of this material collapsed. The better stability of the materials obtained with PHMPT-C10 is probably because of the

(34) (a) Rottman, C.; Ottolenghi, M.; Zusman, R.; Lev, O.; Smith, M.; Gong, G.; Kagan, M. L.; Avnir, D. *Mater. Lett.* **1992**, *13*, 293. (b) Yang, L.; Saavedra, S. S. *Anal. Chem.* **1995**, *67*, 1307.
(35) Nicole, L.; Boissiere, C.; Grosso, D.; Hesemann, P.; Moreau, J.; Sanchez, C. *Chem. Commun.* **2004**, 2312.
(36) (a) Ow, H.; Larson, D.; Srivastava, M.; Baird, B.; Webb, W.; Wiesner, U. *Nano Lett.* **2005**, *5*, 113. (b) Burns, A.; Sengupta, P.; Zedayko, T.; Baird, B.; Wiesner, U. *Small* **2006**, *2*, 723. (c) Loo, C.; Lin, A.; Hirsch, L.; Lee, M.-H.; Barton, J.; Halas, N.; West, J.; Drezek, R. *Technol. Cancer Res. Treat.* **2004**, *3*, 33. (d) Fattakhova-Rohlfing, D.; Wark, M.; Rathouský, J. *Chem. Mater.* **2007**, *19*, 1640.
(37) Ferrer, M. L.; Bekiari, V.; Lianos, P. *Chem. Mater.* **1997**, *9*, 2652.
(38) Spray, R. L.; Choi, K. S. *Chem. Commun.* **2007**, 3655.
(39) Bass, J. D.; Grosso, D.; Boissiere, C.; Belamie, E.; Coradin, T.; Sanchez, C. *Chem. Mater.* **2007**, *19*, 4349.

ordered mesostructure and a quite basic medium in the pores generated by the high loading of the functional surfactants.[39] Such structural integrity results are fundamental for the use of these materials for biological applications.

Conclusions

In summary, we have demonstrated the novel synthesis of mesoscopically ordered pH-responsive hybrid materials through a hierarchical self-assembly process. Two cationic surfactants with a special functional chromophoric group at one end of a carbon chain and a trimethylammonium headgroup at the other end have been synthesized and used as both structure-directing agents and functional nano building blocks. When PHMPT-C10 serves as the structure-directing agent, micrometer-sized particles with a two-dimensional hexagonal mesostructure are formed, whereas the cationic surfactant PYMPT-C10 can yield spherical particles with a wormlike mesostructure. Both of these nanocomposite particles with different mesostructures exhibit strong fluorescence, pH-responsive properties, and a rapid and recyclable signal response. Significantly, the symmetry of the self-assembly architecture demonstrated here affords precise molecular-scale control over the spatial distribution of the organic component in the mesoscopically ordered inorganic network, which endows the hierarchical materials with mechanical robustness, improved thermal stability, and faster responses to chemical stimuli. Furthermore, to put such hybrid materials into practice, the further fabrication of mesostructured thin films would be technologically more suitable for optical sensing devices.[5e,40] This apparent decoupling of function and assembly information within hierarchical architectures leads us to infer that it should readily be possible to substitute the chromophores for alternative groups, with functionalities suited to a wide range of tasks. This ability to rapidly achieve self-assembled structures with diverse morphologies will obviously be important in the production of a family of optoelectronic materials, creating novel platforms for sensors, optical switches, and other device applications.

Acknowledgment. We gratefully acknowledge financial aid from NSFC (Grants 20221101, 20771009, 20490213, and 20423005), the Beijing Natural Science Foundation (Grant 2082007), and the Research Fund for the Doctoral Program of Higher Education of the MOE of China.

Supporting Information Available: More results obtained by means of TG−DTA and XRD for mesostructured composite particles. This material is available free of charge via the Internet at http://pubs.acs.org.

CM800293Y

(40) Lu, Y. F.; Ganguli, R.; Drewien, C. A.; Anderson, M. T.; Brinker, C. J.; Gong, W.; Guo, Y.; Soyez, H.; Dunn, B.; Huang, M. H.; Zink, J. I. *Nature* **1997**, *389*, 364.